

Optical Features of Vapor-Phase Epitaxial Re-Grown Long Semiconducting Single-Walled Carbon Nanotubes

Pavel V. Fedotov,* Alexander I. Chernov, Ekaterina A. Obraztsova, and Elena D. Obraztsova

The monodispersed long single-wall carbon nanotubes (SWCNTs) with controlled morphology are promising in various research fields and many applications, such as optoelectronics, nanoelectronics and recently upon utilizing them as nanoreactors. In this work the long aligned semiconducting single-walled carbon nanotubes as well as the extended semiconducting nanotube networks are synthesized via a vapor-phase epitaxial (VPE) cloning growth method. The semiconducting nanotubes are grown on ST-cut quartz substrates using acetylene and ethanol as a precursors from the seeds of sorted SWCNTs. According to the conducted study the length of the grown nanotubes can reach up to 70 μm . The extensive optical study confirms the preservation of SWCNTs chirality during re-growth from nanotube seeds and the high quality of the obtained long semiconducting nanotubes. Polarization dependent Raman demonstrates the high alignment degree of the re-grown SWCNTs. In dense growth regime SWCNTs demonstrate strong Raman response due to the smaller amount of defects. Such networks of SWCNTs can be a good candidate for optoelectronic applications.

1. Introduction

The chirality control of single-walled carbon nanotube (SWCNT) upon synthesis is an important issue due to the strong variation of nanotube electronic and optical properties depending on its structure.^[1–3] In order to implement successfully carbon nanotubes in optoelectronics and nanoelectronics one needs to have a control over a nanotube conductivity type (semiconducting/metallic), length and assembly morphology (aligned nanotube array/nanotube percolating network). Much effort has been put into chirality selective chemical vapor deposition (CVD)

synthesis of SWCNTs.^[4–11] Significant progress was achieved in developing various SWCNT sorting methods.^[12–18] However, controlling simultaneously chirality of produced nanotubes and morphology of nanotube assembly is still a challenging task. One of the ways to obtain the desired level of the SWCNT structure control is a vapor-phase epitaxial (VPE) growth method.^[19–21] SWCNTs VPE growth is based on a re-growth of nanotube short seeds ideally with preservation of nanotube chirality (cloning regime).^[19] It was demonstrated that one can obtain long carbon nanotubes with chirality preserved for several SWCNT species.^[20] It is also possible to obtain a nanotube array alignment upon using the certain type of substrates like ST-cut quartz.^[20,21] However, the preservation of chirality of various SWCNT species upon re-growth process should be further studied in detail. Investigation of nanotube arrays alignment

as well as the quality of produced SWCNTs should be performed and improved in order to use the advantages of long identical nanotubes.

In this work we show the formation of long individual and bundled aligned semiconducting SWCNTs as well as a network of long semiconducting SWCNTs containing no additional catalyst for growth. The high quality of obtained nanotubes was confirmed by Raman spectroscopy. The optical study demonstrates preservation of SWCNT chirality during re-growth from nanotube seeds and a low defects amount. The polarization dependent Raman data reveal the high alignment degree of SWCNTs for the single tube growth regime.

Dr. P. V. Fedotov, Dr. A. I. Chernov, Dr. E. A. Obraztsova,
Dr. E. D. Obraztsova
A.M. Prokhorov General Physics Institute of Russian Academy of Sciences
38 Vavilov Street, 119991 Moscow, Russia
E-mail: fedotov@physics.msu.ru

Dr. A. I. Chernov, Dr. E. A. Obraztsova
National Research Nuclear University MEPhI (Moscow Engineering Physics Institute)
115409 Moscow, Russia

Dr. P. V. Fedotov, Dr. E. D. Obraztsova
Moscow Institute of Physics and Technology
9 Institutskiy per., Dolgoprudny, Moscow Region 141701, Russia

DOI: 10.1002/pssb.201800602

2. Experimental Section

As-grown HiPCO nanotubes were sorted over conductivity type via a gel chromatography method to form semiconducting SWCNT seeds.^[15,16] In brief, SWCNTs were dispersed in a sodium dodecyl sulfate (SDS) aqueous solution by tip sonication followed by ultracentrifugation. The stable SWCNT dispersion was poured through Sephacryl-gel column and subsequently the semiconducting nanotube fraction was extracted with the SC surfactant aqueous solution. The sorted SWCNTs were deposited on ST-cut quartz substrates via a spin-coating

technique. This nanotube deposition method was found to be the most fast and clean of residual surfactants. To tune the nanotube seeds density on a substrate the concentration of SWCNTs in dispersion was varied.

The substrates with nanotube seeds were dried and cleaned of residual surfactants during two steps: the annealing in a mild Ar flow at 800 °C and the annealing in air at 250 °C for 30 min.

To activate SWCNT seeds the samples were pre-treated with water vapor using a carrier gas consisting of Ar and H₂ (300 and 60 sccm, respectively) at 400 °C for 3–5 min. During the temperature ramping up stage a constant flow of H₂ (60–100 sccm) was introduced to ensure the H-passivation of nanotube tips. Typically the re-growth of SWCNTs was carried out at 850 °C for 15 min. using acetylene (5–15 sccm) and mixture of bubbled ethanol and water (ratio 4:1, respectively) kept at 0 °C with a carrier gas consisting of Ar and H₂ (300 sccm).

Multiple optical techniques were used for SWCNT characterization. The optical absorption spectra were measured in a 5 mm path length quartz cuvette using the UV-vis-NIR double-lined spectrophotometer (Perkin-Elmer Lambda 950). The spectral resolution was 0.5 nm in the 200–1500 nm (6.2–0.82 eV) spectral range. The photoluminescence (PL) excitation maps were recorded with a Horiba Jobin-Yvon “NanoLog-4” system supplied with an InGaAs IR detector (850–1600 nm). For the PL excitation maps the step between the excitation lines was 4 nm, while the total range was 300–800 nm. To identify SWCNTs chirality types the PL measurements were fitted using the previously reported procedures.^[22,23]

The Raman study was performed with a LabRAM HR Evolution spectrometer equipped with HeNe laser 632.8 nm (1.96 eV) and diode laser 532 nm (2.33 eV). The spectral resolution was 0.5 cm⁻¹. Additional Raman measurements were carried out using Ar ion laser with operating wavelengths of 488 nm (2.54 eV) and 514.5 nm (2.41 eV). The spectral resolution was 1 cm⁻¹.

The polarization dependent Raman measurements were performed with a Renishaw in via spectrometer using the 532 nm laser light. A half-wave plate was used to rotate the polarization of the incident light. The measurements were performed in the VV configuration, where the incident light is parallel to the scattered light.

3. Results and Discussion

To obtain high purity semiconducting SWCNT seeds, HiPCO nanotubes were sorted over a conductivity type via a gel chromatography method. The high efficiency of sorting was confirmed via combined optical methods. The photoluminescence excitation (PLE) spectral map of obtained semiconducting SWCNT seeds is presented in Figure 1.

Peaks on PLE map can be assigned to SWCNTs of particular chirality using common procedures.^[22,23] We identified multiple semiconducting nanotube chiralities which are typical to HiPCO nanotubes: (9,4), (7,6), (10,2), (8,6), (8,4), (6,5), (7,5), (8,3), (9,5) and other. The nanotube diameter range for identified SWCNT chiralities is 0.65–1.1 nm. For sorted nanotubes one can observe strong suppression of optical absorption in the spectral range related to metallic SWCNTs though this range is partially

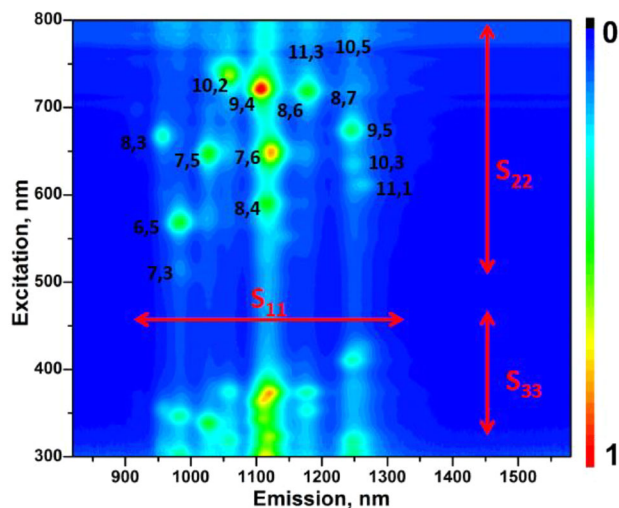


Figure 1. The photoluminescence excitation spectral map of semiconducting SWCNTs used as seeds for the VPE re-growth of nanotubes.

overlapping with the range related to semiconducting nanotubes (Figure 2). We assigned all the features in the absorption spectra to S₁₁, S₂₂, S₃₃ excitonic transitions of semiconducting nanotubes evaluated from PLE map. By fitting the optical absorption spectrum (Figure S1, Supporting Information) using common procedures we show that the sorting purity of the obtained semiconducting SWCNT seeds is high and estimate the quantity of residual metallic nanotubes to be below optical quantification limits, roughly less than 1%.^[24,25]

The advantages of using ST-cut quartz as a substrate and a drop-casting method of depositing nanotube seeds for the VPE growth of SWCNT have been reported by several groups. The high smoothness of the annealed in air ST-cut quartz (roughness is less than 1 nm) is beneficial for the growth of long nanotubes. However, the procedure of drop-casting deposition of nanotube seeds can take hours (or even days) and results in significant

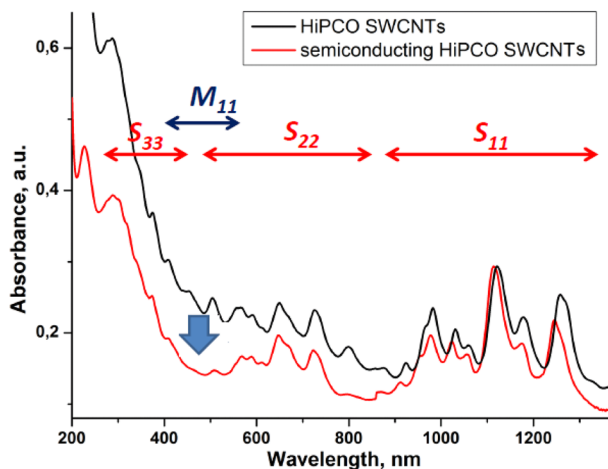


Figure 2. The optical absorption spectra of semiconducting SWCNTs (red) sorted from HiPCO SWCNTs (black) via a gel chromatography method.

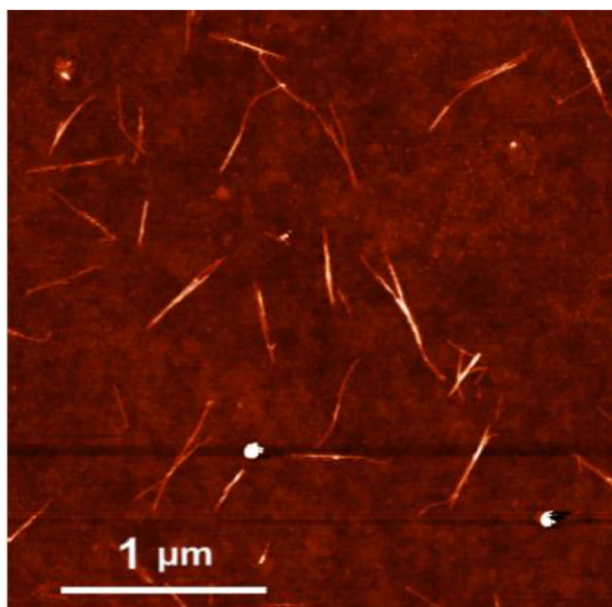


Figure 3. The AFM image of semiconducting SWCNT seeds deposited on ST-cut quartz *via* a spin-coating technique.

amount of residual surfactants. We found that spin-coating technique of depositing nanotubes on a substrate is more promising as it is significantly faster (few minutes) and noticeably cleaner in terms of residual surfactants. The typical AFM image of SWCNT seeds deposited *via* a spin-coating technique is presented in **Figure 3**. According to microscopy study the nanotube seeds do not exceed 0.5 μm in length which is expected as SWCNTs were separated and undergone a tipsonication procedure. Applying a spin-coating technique the density of nanotube seeds can be controlled either by tuning the parameters of spin-coating or by tuning the concentration of SWCNTs in a suspension which we found to be more convenient.

By tuning concentration of nanotubes in suspension on the pre-depositing stage we developed the two typical regimes of SWCNT VPE growth. When the density of nanotube seeds is low – one can obtain long aligned SWCNTs or nanotube bundles (**Figure 4a**) (the long individual nanotube growth regime was obtained). The typical concentration of nanotubes in suspension is below 0.1 mg ml^{-1} . The re-grown nanotube length can exceed 70 μm .

When the density of nanotube seeds is high – one can obtain conjugated networks of long SWCNTs. The typical concentration of nanotubes in suspension in this case is above 1 mg ml^{-1} (**Figure 4b**). The typical lateral size of such networks can exceed hundreds of microns. We assume that the size of nanotube network is basically limited by the area of high density nanotube seeds. The typical SEM image of re-grown semiconducting SWCNTs network is presented in **Figure 5**.

The re-grown semiconducting SWCNTs have fine high intensity Raman features (**Figure 6** and **Figure S2**, Supporting Information). Typically the D/G ratio is very small below 0.04 (at 632.8 nm excitation) and below 0.06 (at 532 nm excitation)

which implies a low defect concentration in re-grown nanotubes. The D/G ratio of re-grown SWCNTs is even lower than in nanotube seeds which is typically 0.06 (at 632.8 nm excitation) and 0.09 (at 532 nm excitation). We attribute such results not to healing of nanotube seeds but rather to elongation. The tips of a nanotube are natural defect sites that contribute to the D-mode intensity and, therefore, one can expect smaller D/G ratio for a longer nanotube. The re-grown SWCNTs have multiple RBM peaks related to different nanotube chiralities. Based on multi-wavelength Raman study one can notice that all the chiralities of SWCNTs identified from RBM of the re-grown nanotubes are present in the deposited semiconducting nanotube seeds. We did not register new RBMs in the re-grown nanotubes. So we assume that the cloning regime of nanotube growth was successfully achieved.

At the same time the relation between intensities of RBMs assigned to different nanotube chiralities is slightly altered. The near armchair SWCNT chiralities especially (9,8), (8,7), and (6,4) have higher intensity RBMs for the re-grown nanotubes. We attribute such effect to the difference in the growth speed of SWCNTs of different chiralities which is in agreement with previously reported results. Other equal armchair and near armchair SWCNT chiralities have higher growth speed as they

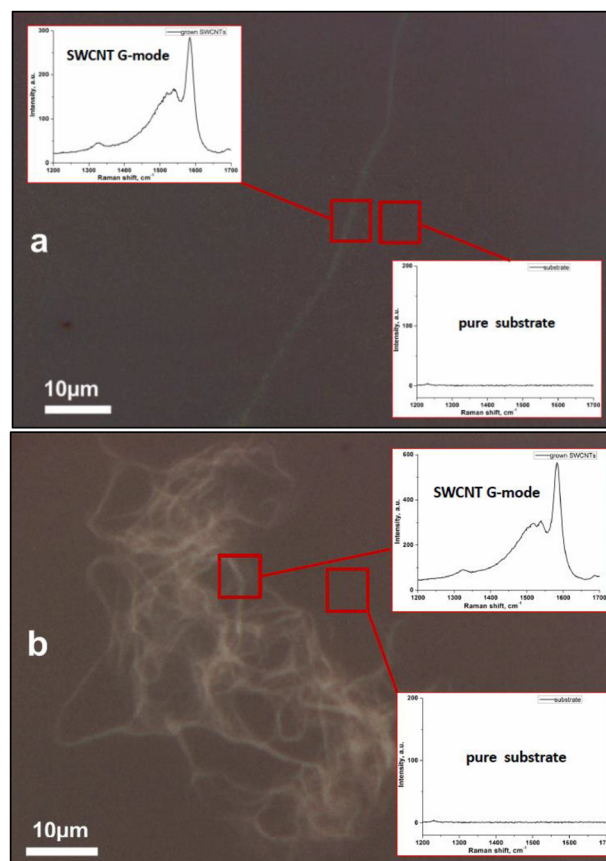


Figure 4. The optical image of a long semiconducting SWCNTs bundle (a) and extended semiconducting SWCNTs network (b). In the insets – typical Raman spectra recorded from the particular spot.

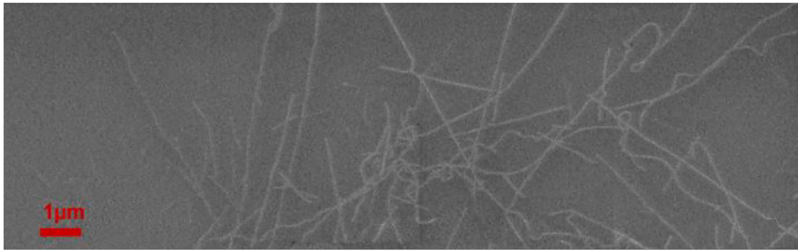


Figure 5. The SEM image of the semiconducting SWCNT network re-grown from the high density nanotube seeds.

do have relatively more active sites for acetylene molecules to incorporate into nanotubes. As a result, such nanotube species can reach higher overall length.

In case of the low density SWCNTs seeds regime one can obtain highly aligned nanotubes, being individual or within a nanotube bundle. The alignment of re-grown nanotube on microscopic level was confirmed via a polarization dependent Raman study. The typical Raman spectra of the

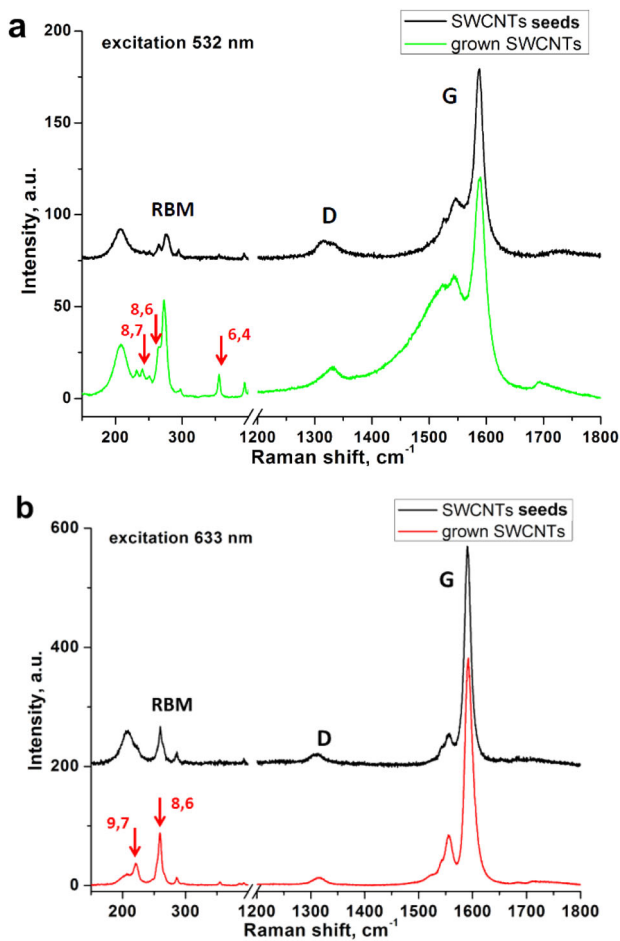


Figure 6. The typical Raman spectra of the re-grown semiconducting SWCNTs comparing with spectra of the nanotube seeds. The spectra are normalized to G-mode intensity: excitation 532 nm (a) and excitation 633 nm (b).

synthesized aligned nanotubes under different orientation of polarized light in the relation to direction of SWCNT alignment are presented in Figure 7a. The light polarization dependent G-mode intensity diagram is presented in Figure 7b. The intensity of the Raman signal for our experimental configuration can be given as

$$I(\theta) = A_1 \int_{-\pi/2}^{\pi/2} A_2 \exp\left(-\frac{\varphi^2}{2\sigma^2}\right) \cos^4(\theta - \varphi) d\varphi$$

where θ is the angle between the predominant nanotube alignment direction and the incident light polarization, while ϕ is the angle between the nanotube axis orientation and the incident light polarization, and σ is the half-width

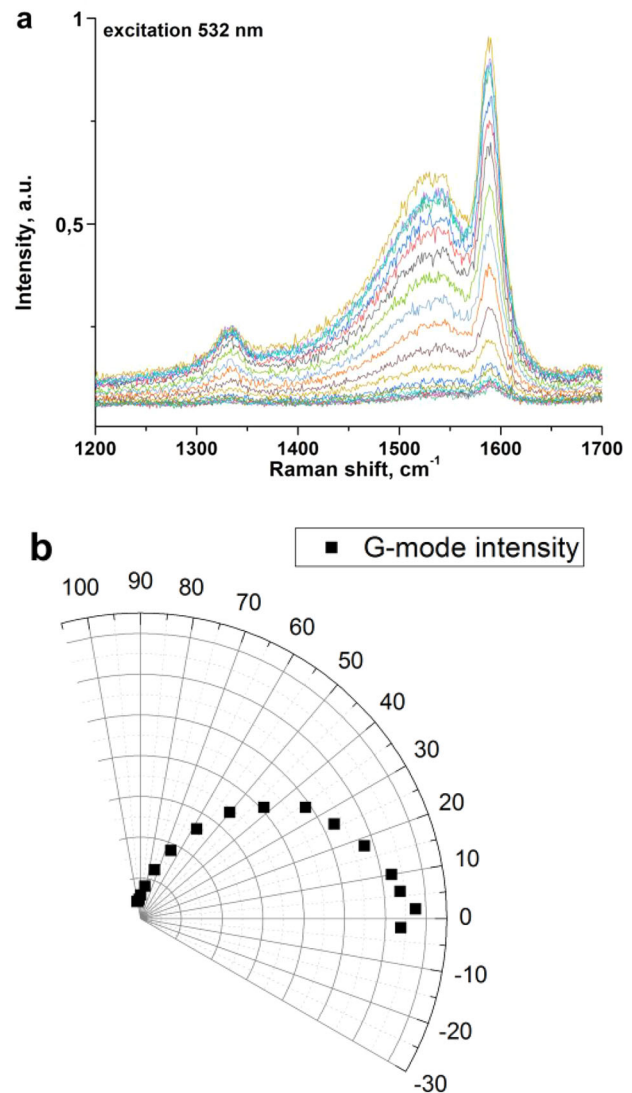


Figure 7. The Raman spectra of the re-grown aligned semiconducting SWCNTs under different light polarization (a) and the G-mode intensity diagram depending on the light polarization angle (b).

Gaussian angular distribution of the alignment.^[26,27] Performing the fit gives the values of σ that equals 7–9 degrees, depending on the test spot. The quality of alignment is similar to the self-assembly methods and epitaxial growth on the terrace substrates.^[27] The re-grown semiconducting SWCNTs demonstrate the high alignment that is attributed to the growth direction that is favored along the st-quartz terraces. However, the dense seeds concentration results in the formation of dense nanotube networks that loss the alignment.

To our knowledge this is the first time conjugated networks of long semiconducting SWCNTs were synthesized via a Vapor Phase Epitaxial method. We attribute the obtained results to a spin-coating nanotube seeds deposition method and to a mild seeds oxidation treatment. Such combination provides high density SWCNT seeds that are free of surfactants. We also highlight the importance of etching agent for defect free re-growth of long nanotube networks. In our case we used ethanol and water vapor during the growth stage together with the sufficient amount of the main precursor – acetylene. The long individual semiconducting nanotubes with the strong optical signals can serve as the reference model for the testing of the excitonic properties of hybrid materials created by filling channels of SWCNTs.^[28,29]

4. Conclusions

The long aligned semiconducting single-walled carbon nanotubes as well as extended semiconducting nanotube networks were synthesized via a vapour-phase epitaxial (VPE) cloning growth method. The length of the re-grown semiconducting SWCNTs can reach 70 μm while the lateral size of semiconducting SWCNTs networks exceeds several hundred μm . The high purity and quality of semiconducting nanotubes were confirmed based on Raman study: a high intensity SWCNTs G mode and RBMs, no evidence of metallic features, a low D/G ratio. The high alignment degree of re-grown semiconducting SWCNTs on micro scale was confirmed via a polarization dependent Raman data demonstrating the characteristic alignment angle of 7–9 degrees.

Supporting Information

Supporting Information is available from the Wiley Online Library or from the author.

Acknowledgements

This work was supported by RSF 17-72-10154. Polarization measurements were performed in terms of RFBR 18-02-01099, we thank Prof. Alexander Grueneis for the experimental facility. A. I. C. acknowledges the support by the Alexander von Humboldt Foundation.

Conflict of Interest

The authors declare no conflict of interest.

Keywords

aligned nanotube arrays, carbon nanotube cloning, long carbon nanotubes, semiconducting carbon nanotubes, single-walled carbon nanotubes, vapour-phase epitaxy

Received: October 17, 2018

Revised: January 10, 2019

Published online:

- [1] J. W. G. Wilder, L. C. Venema, A. G. Rinzler, R. E. Smalley, C. Dekker, *Nature* **1998**, 391, 59.
- [2] R. Saito, G. Dresselhaus, M.S. Dresselhaus, Physical Properties of Carbon Nanotubes, *Imperial College Press* **1998**.
- [3] A. Loiseau, *Understanding Carbon Nanotubes: From Basics to Applications*, Springer-Verlag, Berlin, Heidelberg **2006**.
- [4] S. M. Bachilo, L. Balzano, J. E. Herrera, F. Pompeo, D. E. Resasco, R. B. Weisman, *J. Am. Chem. Soc.* **2003**, 125, 11186.
- [5] G. Lolli, L. Zhang, L. Balzano, N. Sakulchaicharoen, Y. Tan, D. E. Resasco, *J. Phys. Chem. B* **2006**, 110, 2108.
- [6] B. Wang, C. H. P. Poa, L. Wei, L.-J. Li, Y. Yang, Y. Chen, *J. Am. Chem. Soc.* **2007**, 129, 9014.
- [7] F. Yang, X. Wang, D. Zhang, J. Yang, D. Luo, Z. Xu, J. Wei, J. Q. Wang, Z. Xu, F. Peng, X. Li, R. Li, Y. Li, M. Li, X. Bai, F. Ding, Y. Li, *Nature* **2014**, 510, 522.
- [8] M. He, H. Jiang, B. Liu, P. V. Fedotov, A. I. Chernov, E. D. Obratsova, F. Cavalca, J. B. Wagner, T. W. Hansen, I. V. Anoshkin, E. A. Obratsova, A. V. Belkin, E. Sairanen, A. G. Nasibulin, J. Lehtonen, E. I. Kauppinen, *Sci. Rep.* **2013**, 3, 1460.
- [9] M. He, H. Jiang, I. Kauppinen, P. V. Fedotov, A. I. Chernov, E. D. Obratsova, F. Cavalca, J. B. Wagner, T. W. Hansen, J. Sainio, E. Sairanen, J. Lehtonen, E. I. Kauppinen, *J. Mater. Chem. A* **2014**, 5883.
- [10] M. He, P. V. Fedotov, A. I. Chernov, E. D. Obratsova, H. Jiang, N. Wei, H. Cui, J. Sainio, W. Zhang, H. Jin, M. Karppinen, E. I. Kauppinen, A. Loiseau, *Carbon* **2016**, 108, 521.
- [11] M. He, X. Wang, L. Zhang, Q. Wu, X. Song, A. I. Chernov, P. V. Fedotov, E. D. Obratsova, J. Sainio, H. Jiang, H. Cui, F. Ding, E. Kauppinen, *Carbon* **2018**, 128, 249.
- [12] M. S. Arnold, A. A. Green, J. F. Hulvat, S. I. Stupp, M. C. Hersam, *Nature Nanotechnol.* **2006**, 1, 60.
- [13] S. Ghosh, S. M. Bachilo, R. B. Weisman, *Nature Nanotechnol.* **2010**, 5, 443.
- [14] M. Zheng, A. Jagota, E. D. Semke, B. A. Diner, R. S. McLean, S. R. Lustig, R. E. Richardson, N. G. Tassi, *Nature Mater.* **2003**, 2, 338.
- [15] T. Tanaka, Y. Urabe, D. Nishide, H. Kataura, *Appl. Phys. Express* **2009**, 2, 125002.
- [16] H. Liu, T. Tanaka, Y. Urabe, H. Kataura, *Nano Lett.* **2013**, 13, 1996.
- [17] C. Y. Khripin, J. A. Fagan, M. Zheng, *J. Am. Chem. Soc.* **2013**, 135, 6822.
- [18] V. A. Eremina, P. A. Obratsov, P. V. Fedotov, A. I. Chernov, E. D. Obratsova, *Phys. Status Solidi B* **2017**, 254, No. 5, 1600659.
- [19] Y. Yao, C. Feng, J. Zhang, Z. Liu, *Nano Lett.* **2009**, 9, 1673.
- [20] J. Liu, C. Wang, X. Tu, B. Liu, L. Chen, M. Zheng, C. Zhou, *Nature Commun.* **2012**, 3, 1199.
- [21] H. Wang, C. Yamada, J. Liu, B. Liu, X. Tu, M. Zheng, C. Zhou, Y. Homma, *Carbon* **2015**, 95, 497.
- [22] J.-D. R. Rocha, S. M. Bachilo, S. Ghosh, S. Arepalli, R. B. Weisman, *Anal. Chem.* **2011**, 83, 7431.
- [23] A. I. Chernov, P. V. Fedotov, H. E. Lim, Y. Miyata, Z. Liu, K. Sato, K. Suenaga, H. Shinohara, E. D. Obratsova, *Nanoscale* **2018**, 10, 2936.

- [24] M. Pfohl, D. D. Tune, A. Graf, J. Zaumseil, R. Krupke, B. S. Flavel, *ACS Omega* **2017**, 2, 1163.
- [25] A. I. Chernov, E. D. Obraztsova, *Phys. Rev. B* **2009**, 246, 2477.
- [26] M. Ichida, S. Mizuno, H. Kataura, Y. Achiba, A. Nakamura, *Appl. Phys. A* **2004**, 78, 1117.
- [27] N. R. Arutyunyan, A. I. Chernov, E. D. Obraztsova, *Phys. Status Solidi B* **2010**, 247, 2814.
- [28] D. I. Levshov, R. Parret, H.-N. Tran, T. Michel, T. T. Cao, V. C. Nguyen, R. Arenal, V. N. Popov, S. B. Rochal, J.-L. Sauvajol, A.-A. Zahab, M. Paillet, *Phys. Rev. B* **2017**, 96, 195410.
- [29] A. I. Chernov, P. V. Fedotov, I. V. Anoshkin, A. G. Nasibulin, E. I. Kauppinen, V. L. Kuznetsov, E. D. Obraztsova, *Phys. Status Solidi B* **2014**, 12, 2472.